Equivalence between the mobility edge of electronic transport on disorderless networks and the onset of chaos via intermittency in deterministic maps

M. Martínez-Mares[1] and A. Robledo[2]

[1]*Departamento de Física, Universidad Autónoma Metropolitana–Iztapalapa, A. P. 55-534, 09340 México, Distrito Federal, Mexico*
[2]*Instituto de Física, Universidad Nacional Autónoma de México, A. P. 20-364, 01000 México, Distrito Federal, Mexico*

We exhibit a remarkable equivalence between the dynamics of an intermittent nonlinear map and the electronic transport properties (obtained via the scattering matrix) of a crystal defined on a double Cayley tree. This strict analogy reveals in detail the nature of the mobility edge normally studied near (not at) the metal-insulator transition in electronic systems. We provide an analytical expression for the conductance as a function of the system size that at the transition obeys a q-exponential form. This manifests as power-law decay or few and far between large spike oscillations according to different kinds of boundary conditions.

Occasionally the detection of a deep running analogy between two apparently different physical problems allows for the determination of elusive quantities and understanding of difficult issues. Here, we present a relationship between intermittency and electronic transport. This development brings together fields of research in nonlinear dynamics and condensed-matter physics. Specifically, the dynamics at the onset of chaos appears associated with the critical conductance at the mobility edge of regular self-similar networks [1].

Recently, the dynamics at the transitions to chaos that occurs along the three known universal routes from regular to irregular behavior (in low-dimensional nonlinear maps) has been analyzed with a good deal of detail [2–4]. This effort has helped to establish the nature of the statistical-mechanical structure obeyed by the dynamics associated with nonmixing and nonergodic attractors [4]. On the other hand, there are known connections between nonlinear dynamical systems and electronic transport properties. For example, there are models for transport in incommensurate systems, where the Schrödinger equations with quasiperiodic potentials [5] are equivalent to nonlinear maps with a quasiperiodic route to chaos, and where the divergence of the localization length translates into the vanishing of the ordinary Lyapunov coefficient [6].

At the tangent bifurcation [2], the focal point of the intermittency route to chaos, an uncommon but welcome simplicity has led to analytical results in closed form for the dynamics at vanishing Lyapunov exponent [2]. Here, we make the full use of this circumstance showing that transport in a model network, a double Cayley tree—resolved by means of the scattering matrix—is given by the properties of a one-dimensional nonlinear map. The model, in this study, does not contain disorder; nevertheless, it displays a transition between localized and extended states. The translation of the map dynamical features into electronic transport terms provides not only the description of the two different conducting phases but, we believe, offers a rigorous account of the conductance at the mobility edge. A type of localization length in the incipient insulator mirrors the departure from exponential sensitivity to initial conditions at the transition to chaos.

We recap briefly the usefulness of Cayley tree networks in the study of electronic transport properties in the presence, and in the absence, of disorder. A single Cayley tree spans over a space of infinite dimensionality [7] and transport on it exhibits a metal-insulator transition as a function of disorder [8]. A scattering approach was applied in Ref. [9] for off-diagonal disorder and shown that the metal-insulator transition occurs for connectivity $K \geq 2$ ($K+1$ is the coordination number). A single Cayley tree is a first approximation to an ordinary regular lattice [8]; but, as shown below, a double Cayley tree (two single Cayley trees joined conformally as in Fig. 1) is a much better approximation (see also [10]). In Ref. [11] it is shown that the conducting band of a disorderless double Cayley tree contracts and disappears as K increases. In Ref. [12] the dynamic behavior of a chain of scatterers was analyzed in the absence and in the presence of disorder, while the localization transition for different types of complex networks, including the double Cayley tree, was studied in Ref. [13] via spectral statistics. Finally, the double Cayley tree problem is relevant for transport in chaotic cavities with broken mirror symmetry [14]. Here, we show that the electronic structure for $K=2$ can be determined by reducing the scattering matrix to a nonlinear map. This development facilitates the band description of the conductance as a function of energy including the location of the mobility edge.

Here, we consider electronic transport in the double Cayley tree (see Fig. 1). We refer only to the ordered crystal-like system and reduce its associated scattering matrix to a nonlinear map. The number of times the trees are ramified, starting from perfect join, is the generation n that quantifies the size of the system. Also, for brevity, we will fix the tree
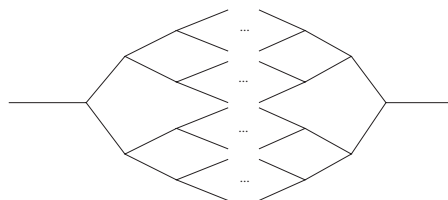

FIG. 1. A double Cayley tree of connectivity $K=2$ and lattice constant a. Each bond is a perfect one-dimensional conductor.

connectivity to $K=2$ where one lead, we call it the incoming lead, is divided into two leads at a given node. The leads are assumed to be equivalent to one-dimensional perfect wires with length equal to the lattice constant a and are independent of n. Hence, each node is described by the same 3×3 scattering matrix for which we assume the model [15]

$$S_{\text{node}} = \begin{bmatrix} -(\alpha+\beta) & \sqrt{\epsilon} & \sqrt{\epsilon} \\ \sqrt{\epsilon} & \alpha & \beta \\ \sqrt{\epsilon} & \beta & \alpha \end{bmatrix}, \tag{1}$$

where ϵ, a real number in the interval $0 \le \epsilon \le \frac{1}{2}$, is the transmission probability (or coupling) from the incoming lead to the others, and vice versa. The reflection amplitude to the incoming lead is $-(\alpha+\beta)$, with $\alpha = -(1 - \sqrt{1-2\epsilon})/2$ and $\beta = (1 + \sqrt{1-2\epsilon})/2$. When the incidence is only on one of the other two leads, α is the reflection amplitude to the same lead and β is the transmission amplitude to the other lead.

The scattering matrix of the system is 2×2 and satisfies a recursive relation. If we denote by S_n the scattering matrix at generation n, the combination rule for scattering matrices allows S_n to be written in terms of the scattering matrix at a previous generation $n-1$,

$$S_n = \frac{-1}{e^{-2ika} \mathbb{1} - \sqrt{1-2\epsilon} S_{n-1}} (\sqrt{1-2\epsilon} e^{-2ika} \mathbb{1} - S_{n-1}), \tag{2}$$

with $\mathbb{1}$ as the 2×2 identity matrix. The scattering matrix at a generation n can be obtained iteratively starting from that for the perfect union in the middle of our double Cayley tree: $S_0 = \sigma_x$, where σ_x is a Pauli matrix.

First, it can be seen that S_n is a unitary matrix, which is the condition of flux conservation. Then, time reversal invariance restricts S_n to be a symmetric matrix. Finally, the additional lattice spatial reflection symmetry implies that S_n has the form [14]

$$S_n = \begin{pmatrix} r_n & t_n \\ t_n & r_n \end{pmatrix}, \tag{3}$$

where r_n and t_n are the reflection and the transmission amplitudes. With this structure S_n is diagonalized by a $\pi/4$ rotation [14]; that is,

$$\begin{pmatrix} e^{i\theta_n} & 0 \\ 0 & e^{i\theta'_n} \end{pmatrix} = \frac{1}{\sqrt{2}} \begin{pmatrix} 1 & 1 \\ -1 & 1 \end{pmatrix} S_n \frac{1}{\sqrt{2}} \begin{pmatrix} 1 & -1 \\ 1 & 1 \end{pmatrix}. \tag{4}$$

Here, θ_n and θ'_n are the eigenphases that satisfy $e^{i\theta_n} = r_n + t_n$ and $e^{i\theta'_n} = r_n - t_n$. In terms of the eigenphases the transmission amplitude is given by $t_n = \frac{1}{2}(e^{i\theta_n} - e^{i\theta'_n})$. Moreover, the dimensionless conductance (i.e., in units of $2e^2/h$) depends on the eigenphases through the Landauer formula as [16,17]

$$g_n = |t_n|^2. \tag{5}$$

Therefore, the analysis of the eigenphases is of crucial importance as they determine every transport property.

Central to our discussion is the fact that the recursive relation (2) can be written in the diagonal form (4) and this
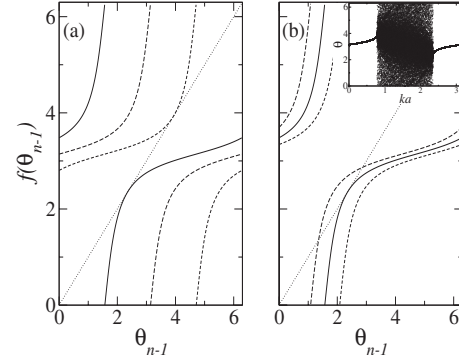

FIG. 2. $f(\theta_n)$ of Eq. (6) for $\epsilon = \frac{1}{4}$: (a) $ka = \pi/4$ (dashed line), $2\pi/4$ (long dashed line), and $3\pi/4$ (continuous line) and (b) $ka = 2.6$ (long dashed line), $3\pi/4$ (continuous line), and 2.1 (dashed line). The dotted lines correspond to the identity. Inset: periodic and chaotic attractors.

implies the existence of a one-dimensional nonlinear map for the phase θ_n. The map $\theta_{n+1} = f(\theta_n)$ can actually be obtained in the following closed form:

$$f(\theta_n) = 2ka - \theta_n + 2 \arctan\left(\frac{\sin \theta_n + \sqrt{1-2\epsilon} \sin 2ka}{\cos \theta_n - \sqrt{1-2\epsilon} \cos 2ka} \right), \tag{6}$$

where the dependence on ϵ and ka comes out clearly. In what follows everything said about θ_n is valid for θ'_n as well. Perfect union at $n=0$ means $\theta_0 = 0$ and $\theta'_0 = \pi$.

For a given value of ϵ, map (6) is periodic in ka (the parameter related to the energy) with period π. In the range $0 \le ka \le \pi$ the attractor diagram presents a chaotic region between two windows of period 1 [see inset of Fig. 2(b)], separated by bifurcation points at

$$k_c a = \arccos\sqrt{2\epsilon}, \quad k_{c'} a = \pi - \arccos\sqrt{2\epsilon}, \tag{7}$$

such that the chaotic region of the map takes place in the interval $k_c a < ka < k_{c'} a$, while windows of period 1 take place in $ka \le k_c a$ and $ka \ge k_{c'} a$. As we see below Eq. (7) gives the locations of the mobility edge as a function of the transmission probability ϵ. Fixed-point solutions θ_∞ for θ_n, $n \to \infty$, are

$$\theta_\infty = \begin{cases} \theta_- & \text{for } 0 \le ka \le k_c a \\ \theta & \text{for } k_c a < ka < k_{c'} a \\ \theta_+ & \text{for } k_{c'} a \le ka \le \pi, \end{cases} \tag{8}$$

where $\theta = -ka + 3\pi/2$ and $\theta_\pm$ is given by

$$\tan \theta_\pm = \frac{\sin ka(\cos ka \pm \sqrt{\cos^2 ka - 2\epsilon})}{1 - \cos ka(\cos ka \pm \sqrt{\cos^2 ka - 2\epsilon})}. \tag{9}$$

These fixed-point solutions indicate that, for large n, θ_n reaches the values $\theta_\pm$ in the windows of single period, while in the chaotic region θ_n fluctuates according to an invariant density with maximum at θ.

At the bifurcation points $k_c a$ and $k_{c'} a$, the fixed-point phase θ_∞ takes the critical values $\theta_c = -\arccos\sqrt{2\epsilon} + 3\pi/2$ and $\theta_{c'} = \arccos\sqrt{2\epsilon} + \pi/2$, respectively, for θ_∞ between 0 and 2π.

In Fig. 2(a) we plot map (6) for $\epsilon = 1/4$ for the three parameter values $ka = \pi/4, 2\pi/4, 3\pi/4$. It is evident that the transitions from chaotic behavior to the windows of period 1 are tangent bifurcations as the map is tangent to the identity line [2] at the critical values $k_c a = \pi/4$ and $k_{c'} a = 3\pi/4$, where $\theta_c = 5\pi/4$ and $\theta_{c'} = 3\pi/4$. Figure 2(b) shows three cases: secant ($ka = 2.6$) and tangent ($ka = 3\pi/4$) period 1 solutions and a bottleneck ($ka = 2.1$) that gives rise to intermittency as a precursor to periodic behavior.

Information about transport can be obtained from the sensitivity to initial conditions that characterize the dynamics of the nonlinear map. For *finite n* it is given by

$$\Xi_n \equiv \left| \frac{d\theta_n}{d\theta_0} \right| \equiv \exp[\Lambda_1(n)n], \quad (10)$$

where θ_0 is an initial condition and the exponential law after the second identity defines the finite n Lyapunov exponent $\Lambda_1(n)$. For n large $\Lambda_1(n)$ becomes the Lyapunov exponent λ_1, a number independent of θ_0 that according to its sign characterizes periodic and chaotic attractors. At the tangent bifurcation $\lambda_1 = 0$ and the sensitivity adopts instead a q-exponential form (see below) [2,18]. From Eqs. (5), (6), and (10) [and $t_n = \frac{1}{2}(e^{i\theta_n} - e^{i\theta'_n})$] we obtain the recursion formula

$$g_n = g_{n-1} \exp(\Lambda_1(n)n)\exp(\Lambda'_1(n)n), \quad (11)$$

$$\Lambda_1(n) = \ln \frac{\epsilon}{1 - \epsilon - \sqrt{1 - 2\epsilon} \cos(\theta_n + 2ka)}, \quad (12)$$

where $\Lambda'_1(n)$ is given by Eq. (12) with θ_n replaced with θ'_n. We note that Λ_1 and Λ'_1, and hence g_n, do not depend on the initial conditions θ_0 and θ'_0. The Lyapunov exponent λ_1 is given by Eq. (12) with θ_n replaced with θ_∞.

The dynamical properties of map (6) translate into the following network properties: (i) in relation to the attractors of period 1 that take place along $0 \leq ka < k_c a$ and $k_{c'} a < ka \leq \pi$, we corroborate from Eqs. (8) and (12) that λ_1 is negative and therefore the conductance g_n decays exponentially with system size n, $g_n = \exp(2\lambda_1 n)$, implying localization, with the localization length being $\zeta_1 = a/|\lambda_1|$. In the left panel of Fig. 3 we see a clear exponential decay of g_n as a function of n at $ka = 0.5$, where we compare g_n computed directly from Eq. (5) with that obtained from λ_1. We notice that the conductance for the localized states of an ordered system displays the same behavior as that in the insulating regime of a disordered wire in quasi-one-dimensional configuration [19]. (ii) With respect to the chaotic attractors that occur in the interval $k_c a < ka < k_{c'} a$, we observe that λ_1 becomes positive and the recursion relation (11) does not let g_n to decay but makes it oscillate with n (not shown here) indicating that conduction takes place. In our model g_n does not scale with the system size as in the metallic regime of quasi-one-dimensional disordered wire where Ohm's law is satisfied [19]. In the parameter region where the map is incipiently chaotic, say $ka \gtrsim k_c a$, the network grows with n with an insulator character, but interrupted for other intermediate val-
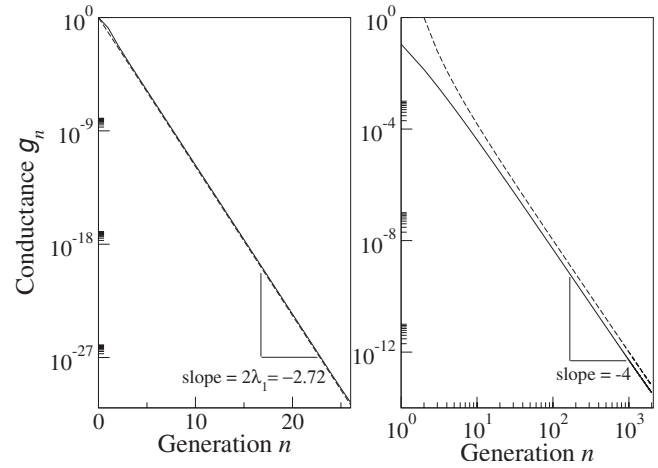

FIG. 3. Conductance as a function of generation for $\epsilon = \frac{1}{4}$: $ka = 0.5$ (left panel) and $ka = \pi/4$ (right panel). Continuous lines represent g_n obtained directly from the map through Eq. (5) while dotted lines correspond to $g_n = \exp(2\lambda_1 n)$ and $g_n = \exp_{3/2}(2\lambda_{3/2} n)$ for left panel and right panel, respectively. The two curves in right panel differ because of a proportionality factor [see Eq. (14)].

ues of n by conducting crystals. In the map dynamics these are the laminar episodes separated by chaotic bursts in intermittent trajectories.

The most distinct outcome of our treatment is the description obtained of the mobility edge from the dynamics at the critical attractors located at $ka = k_{c'} a$ and $ka = k_c a$. There, $\lambda_1 = 0$ and according to Eq. (11) not much can be said about the size dependence of the conductance when $n \gg 1$. However, we can use to our advantage the known properties of the anomalous dynamics occurring at these attractors once they are identified as tangent bifurcations [see Fig. 2(b) for $ka = 3\pi/4$]. At a tangent bifurcation of general nonlinearity $z > 1$ the sensitivity obeys a q-exponential law for large n [2],

$$\xi_n = \Xi_{n \gg 1} = \exp_q(\lambda_q n) \equiv [1 - (q-1)\lambda_q n]^{\mp 1/(q-1)}, \quad (13)$$

where λ_q is a q-generalized Lyapunov coefficient given by $\lambda_q = \mp zu$, $q = 2 - 1/z$, where u is the leading term of the expansion up to order z of θ_n close to θ_c (or $\theta_{c'}$); i.e., $\theta_n - \theta_c = (\theta_{n-1} - \theta_c) + u|\theta_{n-1} - \theta_c|^z + \cdots$. The minus and plus signs in Eq. (13) and in λ_q correspond to trajectories at the left and right, respectively, of the point of tangency θ_c. Equation (13) implies power-law decay of ξ_n with n when $\theta_n - \theta_c < 0$ and faster than exponential growth when $\theta_n - \theta_c > 0$. (We recall that any choice of S_0 other than the Pauli matrix translates into another initial condition for the map). By making the expansion around θ_c (or $\theta_{c'}$) for our map (6) we find (as evidently anticipated) $z = 2$ implying $q = 3/2$, $u = \sqrt{(1 - 2\epsilon)/2\epsilon}$, and the q-generalized Lyapunov exponent is $\lambda_{3/2} = -2\sqrt{(1 - 2\epsilon)/2\epsilon}$. Following the same steps that lead to Eq. (11), the recursion relation for g_n at each bifurcation point takes the form $g_n = g_{n-1} \exp_{3/2}[\Lambda_{3/2}(n)n]\exp_{3/2}[\Lambda'_{3/2}(n)n]$, so that when $\theta_n - \theta_c < 0$ [see Eq. (13)], $g_n = \exp_{3/2}(2\lambda_{3/2} n)$, or

$$g_n \propto \left(1 - \tfrac{1}{2}\lambda_{3/2}n\right)^{-4}. \qquad (14)$$

In the right panel of Fig. 3 we compare the results from Eq. (5) (continuous line) and Eq. (14) (dashed line). It is clear that g_n decays as a power law (with quartic exponent) rather than the exponential in the insulating phase. We emphasize that a localization length given by $\zeta_{3/2}=a/\lambda_{3/2}$ can still be defined at the mobility edge. To our knowledge this property has <u>not been</u> reported before. When $\theta_n - \theta_c > 0$, $\lambda_{3/2} = 2\sqrt{(1-2\epsilon)/2\epsilon} > 0$ and the recursion relation for g_n describes, as the result of the diverging duration of the laminar episodes of intermittency, large n intervals of vanishing g_n between increasingly large spike oscillations.

In summary, we can draw significant conclusions about electronic transport from our study. These arise naturally when considering the dynamical properties of the equivalent nonlinear map near or at the intermittency transition to chaos. Since the iteration time in the map translates into the generation n of the network, time evolution means growth of system size, reaching the thermodynamic limit (and true self-similarity) when $n \to \infty$. In that limit, windows of period 1 separated by a chaotic band correspond, respectively, to localized and extended electronic states. Further, in the referred parameter (ka, ϵ) regions, the conductance g_n of the model crystal shows either an exponential decay with the system size, with localization length given by ζ_1 (as in the case of a quasi-one-dimensional disordered wire [19]), or an oscillating property signaling conducting states. The pair of tangent bifurcation points of the map correspond to the band or mobility edges that separate conductor from insulator behavior. At these bifurcations the sensitivity to initial conditions ξ_n exhibits either power-law decay (when $\theta_0 < \theta_{c'}$ or $\theta_0 > \theta_c$) or faster than exponential increase ($\theta_{c'} < \theta_0 < \theta_c$) and consequently the conductance inherits comparable decay or variability with the system size n. Notably, as we have seen we can still define a localization length, the q-generalized localization length ζ_q with a fixed value of $q=3/2$. This expression is universal, i.e., it is satisfied by all maps that in the neighborhood of the point of tangency have quadratic term, i.e., $z=2$ [2]. This quantity can be obtained directly by the evaluation of g_n [in Eq. (5)] when $n \to \infty$. At the mobility edge $\zeta_1^{-1} = -\lim_{n\to\infty} n^{-1} \ln g_n$ vanishes because $\ln g_n$ no longer decreases linearly with n, as it is the case in the insulating phase. However, the use of $\zeta_q^{-1} = -\lim_{n\to\infty} n^{-1} \ln_q g_n$ leads to a finite number for one particular value of q, $q=3/2$, when the degree of deformation q in the q logarithm restores linear behavior. Otherwise, ζ_q vanishes or diverges. In spite of the unusual features of the double Cayley tree transport model, the complete set of exact solutions derived from it provides a comprehensive picture about nonexponential behavior of central quantities like the conductance at the transition between the insulator and conductor regimes.

[1] We chose to call here mobility edge, usually employed in reference to disordered systems, the transition between localized and extended electronic states in regular self-similar networks.

[2] F. Baldovin and A. Robledo, EPL **60**, 518 (2002).

[3] E. Mayoral and A. Robledo, Phys. Rev. E **72**, 026209 (2005).

[4] A. Robledo and L. G. Moyano, Phys. Rev. E **77**, 036213 (2008).

[5] P. G. Harper, Proc. Phys. Soc., London, Sect. A **68**, 874 (1955).

[6] J. A. Ketoja and I. I. Satija, Physica D **109**, 70 (1997).

[7] J. P. Straley, J. Phys. C **10**, 3009 (1977).

[8] R. Abou-Chacra, P. W. Anderson, and D. J. Thouless, J. Phys. C **6**, 1734 (1973).

[9] B. Shapiro, Phys. Rev. Lett. **50**, 747 (1983).

[10] N. Zekri and A. Brezini, Phys. Status Solidi B **133**, 463 (1986).

[11] Y. Avishai and J. M. Luck, Phys. Rev. B **45**, 1074 (1992).

[12] M. Horvat and T. Prosen, J. Phys. A: Math. Theor. **40**, 11593 (2007).

[13] M. Sade, T. Kalisky, S. Havlin, and R. Berkovits, Phys. Rev. E **72**, 066123 (2005).

[14] M. Martínez and P. A. Mello, Phys. Rev. E **63**, 016205 (2000).

[15] M. Büttiker, Y. Imry, and M. Ya. Azbel, Phys. Rev. A **30**, 1982 (1984).

[16] R. Landauer, J. Phys.: Condens. Matter **1**, 8099 (1989).

[17] M. Büttiker, IBM J. Res. Dev. **32**, 317 (1988).

[18] The q exponential and its inverse, the q logarithm, are defined, respectively, as $\exp_q(x) \equiv [1+(1-q)x]^{1/(1-q)}$ for $x, q \in \mathbb{R}$ and $\ln_q(y) \equiv (y^{1-q}-1)/(1-q)$ for $y \in \mathbb{R}^+$. The ordinary exponential and logarithm are recovered when $q=1$.

[19] C. W. J. Beenakker, Rev. Mod. Phys. **69**, 731 (1997).